Lattice thermodynamics at finite chemical potential from analytical Continuation

IOP Conf. Series: Journal of Physics: Conf. Series **1070** (2018) 012002 doi:10.1088/1742-6596/1070/1/012002

Lattice thermodynamics at finite chemical potential from analytical Continuation

Jana N. Guenther[1,2], Szabolcs Borsanyi[1], Zoltan Fodor[1,3,4], Sandor K. Katz[4], K. K. Szabó[1,3], Attila Pasztor[1],Israel Portillo[5] and Claudia Ratti[5]

1 University of Wuppertal, Department of Physics, Wuppertal D-42097, Germany
2 University of Regensburg,Department of Physics, Regensburg D-93053, Germany
3 Jülich Supercomputing Centre, Jülich D-52425, Germany
4 Eötvös University, Budapest 1117, Hungary
5 University of Houston, Department of Physics, Houston, TX 77204, USA

E-mail: Jana.Guenther@t-online.de

Abstract. An efficient way to study the QCD phase diagram at small finite density is to extrapolate thermodynamical observables from imaginary chemical potential. We present results for fluctuations of baryon number to order $(\mu_B/T)^6$. The results at real chemical potentials are obtained through analytical continuation of simulations at imaginary chemical potentials. We also calculate higher order fluctuations of strangeness and electric charge to obtain the Taylor coefficients of the baryon number fluctuation with vanishing strangeness. We compare to the STAR proton fluctuation data to characterize the chemical freeze-out in view of the lattice results.

1. Introduction

When investigating Quantum Chromodynamics (QCD) an important but challenging goal is the study of the phase diagram. At there chemical potential lattice QCD predicts a smooth crossover between hadrons and the quark gluon plasma [1, 2, 3, 4, 5], taking place in the temperature range $T \simeq 145 - 165$ MeV. Due to the sign problem lattice QCD is unable to study the region with final chemical potential.

With the advent of the second Beam Energy Scan (BESII) at the Relativistic Heavy Ion Collider (RHIC), scheduled for 2019-2020, there is a renewed interest in the heavy ion community towards the phases of QCD at moderate-to-large densities. A rich theoretical effort is being developed in support of the experimental program; several observables are being calculated, in order to constrain the existence and location of the QCD critical point and to observe it experimentally.

Fluctuations of conserved charges (electric charge Q, baryon number B and strangeness S) are important observables for the finite-density investigations. One possible way to extend lattice results to finite density is to perform Taylor expansions of the thermodynamic observables around chemical potential $\mu_B = 0$ [6, 7, 8, 9, 10]: fluctuations of conserved charges are directly related to the Taylor expansion coefficients of such observables. They allow for a comparison between theoretical and experimental results to extract the chemical freeze-out temperature T_f and chemical potential μ_{Bf} as functions of the collision energy [11, 12, 13, 14]. The higher order

fluctuations are also an important signature for the critical endpoint, as they give access to the correlation length [8, 15, 16].

We present results for χ_2^B to χ_6^Bin the temperature range 140 MeV $\leq T \leq$ 220 MeV. Several diagonal and non-diagonal fluctuations of conserved charges up to sixth-order are available in our resent paper [17].

We simulate the lower-order fluctuations at imaginary chemical potential and extract the higher order fluctuations as derivatives of the lower order ones at $\mu_B = 0$. This method has been successfully used in the past and proved to lead to a more precise determination of the higher order fluctuations, compared to their direct calculation [18, 19, 20]. The latter requires the evaluation of several terms and is affected by a signal-to-noise ratio which is decreasing as a power law of the spatial volume V, with an exponent that grows with the order of the susceptibility. Reliable results would therefore require extremely large volumes.

To connect to experimental results, we calculate the ratio of the cumulants of the net-baryon number distribution as functions of temperature and chemical potential by means of their Taylor expansion in powers of μ_B/T. This is possible by combining different diagonal and non-diagonal fluctuations to obtain a result at the strangeness neutral point and with $\langle n_Q \rangle = 0.4 \langle n_B \rangle$.

2. Lattice details

We use a tree-level Symanzik improved gauge action, with four times stout smeared staggered fermions. We simulate $2+1+1$ dynamical quarks where the light flavors are tuned in a way to reproduce the physical pion and kaon mass and we set $\frac{m_c}{m_s} = 11.85$ [21]. For the zero temperature runs we use large volumes which full fill $Lm_\pi > 4$. The scale is determined via f_π. More Details can be found in [22].

The maximal useful value of μ_B is $\mu_B = i\pi T$ because of the Roberge-Weiss transition [23]. We simulate at eight different values of μ_B given as: $\mu_B^{(j)} = iT\frac{j\pi}{8}$ for $j \in \{0, 1, 2, 3, 4, 5, 6, 7\}$. The analysis is done purely on a $48^3 \times 12$ lattice without continuum extrapolation. All simulations are done at $\mu_Q = \mu_S = 0$.

3. Analysis for χ^B

We start with the analysis for $\chi_2^B(T)$, $\chi_4^B(T)$ and $\chi_6^B(T)$. Our goal is to calculate these quantities at zero chemical potential, using the imaginary chemical potential data up to $\chi_B^4(T, \hat{\mu}_B)$. In this work we extract these derivatives at a fixed temperature. Therefor the results for different temperatures are completely independent.

We consider the ensembles at a fixed temperature T. For each value of imaginary $\mu_B \neq 0$ we determine χ_1^B, χ_2^B, χ_3^B and χ_4^B from simulation, while for $\mu_B = 0$ only χ_2^B and χ_4^B can be used, since χ_1^B and χ_3^B are odd functions of μ_B and therefore equal to zero.

We make the ansatz for the pressure:

$$\chi_0^B(\hat{\mu}_B) = c_0 + c_2\hat{\mu}_B^2 + c_4\hat{\mu}_B^4 + c_6\hat{\mu}_B^6 + c_8\hat{\mu}_B^8 + c_{10}\hat{\mu}_B^{10}, \tag{1}$$

where the Taylor expansion coefficients c_n are related to the baryon number fluctuations χ_n^B by: $n!c_n = \chi_n^B$. Our data do not allow for an independent determination of c_8 and c_{10}. Nevertheless, in order to have some control over these terms we make the assumption

$$|\chi_8^B| \lesssim \chi_4^B \tag{2}$$

$$|\chi_{10}^B| \lesssim \chi_4^B \tag{3}$$

or in terms of the c_n coefficients

$$8!c_8 \lesssim 4!c_4$$
$$10!c_{10} \lesssim 4!c_4.$$

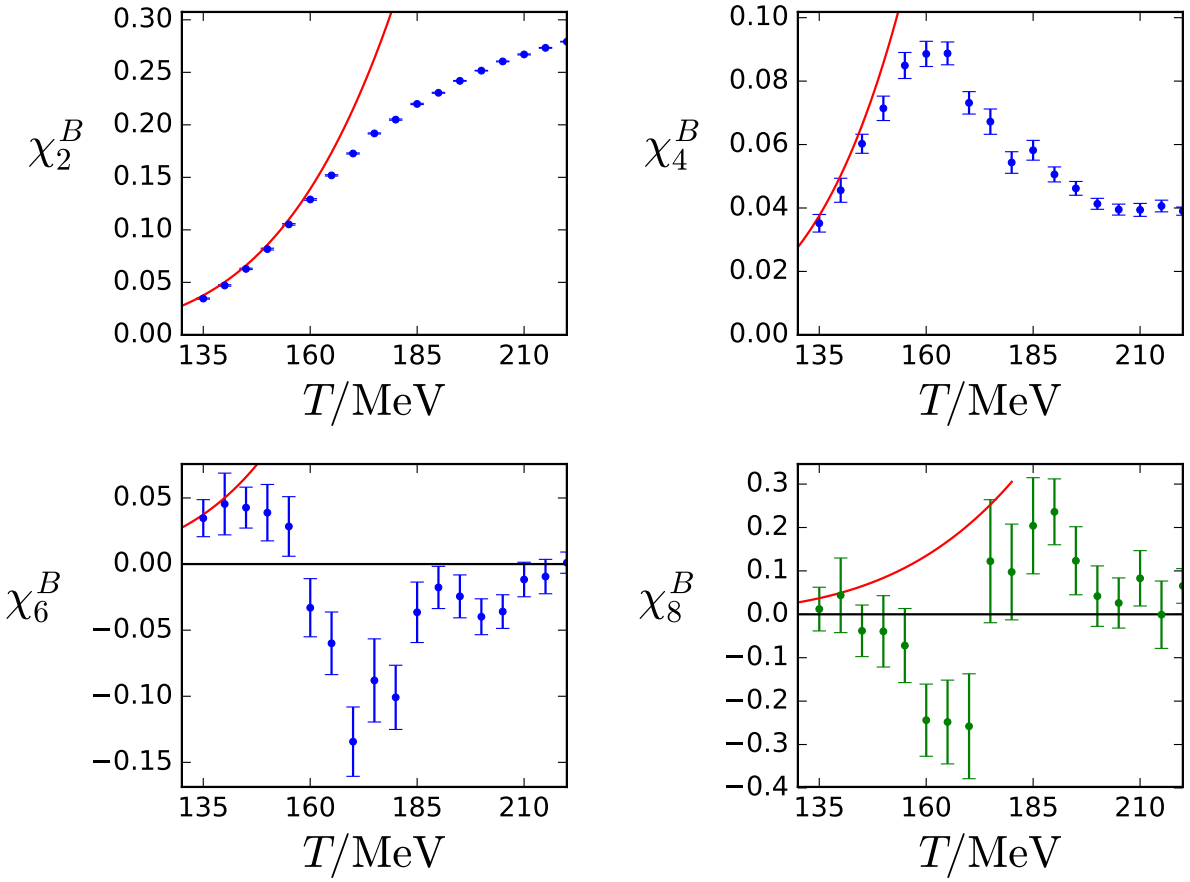

Figure 1. Results for χ_2^B, χ_4^B, χ_6^B and an estimate for χ_8^B as functions of the temperature, obtained from the single-temperature analysis. We plot χ_8^B in green to point out that its determination is guided by a prior, which is linked to the χ_4^B observable by Eq. (4). The red curve in each panel corresponds to the Hadron Resonance Gas (HRG) model result.

We can then rewrite our ansatz as

$$\chi_0^B(\hat{\mu}_B) = c_0 + c_2\hat{\mu}_B^2 + c_4\hat{\mu}_B^4 + c_6\hat{\mu}_B^6 + \frac{4!}{8!}c_4\epsilon_1\hat{\mu}_B^8 + \frac{4!}{10!}c_4\epsilon_2\hat{\mu}_B^{10}. \tag{4}$$

where ϵ_1 and ϵ_2 are drawn randomly from a normal distribution with mean -1.25 and variance 2.75. We use the same distribution for all temperatures. For a detailed discussion of the choice of parameters see [17].

For this ansatz we calculate the following derivatives, which are the actually simulated lattice observables:

$$\chi_1^B(\hat{\mu}_B) = 2c_2\hat{\mu}_B + 4c_4\hat{\mu}_B^3 + 6c_6\hat{\mu}_B^5 + \frac{4!}{7!}c_4\epsilon_1\hat{\mu}_B^7 + \frac{4!}{9!}c_4\epsilon_2\hat{\mu}_B^9 \tag{5}$$

$$\chi_2^B(\hat{\mu}_B) = 2c_2 + 12c_4\hat{\mu}_B^2 + 30c_6\hat{\mu}_B^4 + \frac{4!}{6!}c_4\epsilon_1\hat{\mu}_B^6 + \frac{4!}{8!}c_4\epsilon_2\hat{\mu}_B^8 \tag{6}$$

$$\chi_3^B(\hat{\mu}_B) = 24c_4\hat{\mu}_B + 120c_6\hat{\mu}_B^3 + \frac{4!}{5!}c_4\epsilon_1\hat{\mu}_B^5 + \frac{4!}{7!}c_4\epsilon_2\hat{\mu}_B^7 \tag{7}$$

$$\chi_4^B(\hat{\mu}_B) = 24c_4 + 360c_6\hat{\mu}_B^2 + c_4\epsilon_1\hat{\mu}_B^4 + \frac{4!}{6!}c_4\epsilon_2\hat{\mu}_B^6. \tag{8}$$

We perform a correlated fit for the four measured observables, thus obtaining the values of c_2, c_4 and c_6 for each temperature, and the corresponding χ_2^B, χ_4^B and χ_6^B. We repeat the fit for 1000 random draws for ϵ_1 and ϵ_2. The result is weighted using the Akaike Information Criterion [24]. Through these weights we get a posterior distribution from the prior distribution. Our final estimate for χ_8^B represents this posterior distribution. We do not show the posterior for χ_{10}^B, which is mostly noise.

These results are shown in Fig. 1, together with an estimate of χ_8^B, related to χ_4^B by Eq. (4).

4. Cumulants

For a comparison with heavy ion collision experiments the cumulants of the net baryon distribution are a useful tool. The first four cumulants are the mean M_B, the variance σ_B^2, the skewness S_B and the kurtosis κ_B. By forming appropriate ratios, we can cancel out explicit volume factors. However the measured distributions themselves may still depend on the volume, which one should take into account, when comparing to experiments.

Heavy ion collisions with lead or gold take place with at $\mu_B > 0$, $\langle n_S \rangle = 0$ and $\langle n_Q \rangle = 0.4\langle n_B \rangle$. Since our simulations are done at $\mu_S = \mu_Q = 0$ and $\mu_B \neq 0$ we have to do some calculations to arrive at the same observables that are measured in experiments (see for example [25]). We investigate three different rations of cumulants and write each as a Taylor expansion:

$$\frac{M_B}{\sigma_B^2} = \frac{\chi_1^B(T,\hat{\mu}_B)}{\chi_2^B(T,\hat{\mu}_B)} = \hat{\mu}_B r_{12}^{B,1} + \hat{\mu}_B^3 r_{12}^{B,3} + \dots \tag{9}$$

$$\frac{S_B \sigma_B^3}{M_B} = \frac{\chi_3^B(T,\hat{\mu}_B)}{\chi_1^B(T,\hat{\mu}_B)} = r_{31}^{B,0} + \hat{\mu}_B^2 r_{31}^{B,2} + \dots \tag{10}$$

$$\kappa_B \sigma_B^2 = \frac{\chi_4^B(T,\hat{\mu}_B)}{\chi_2^B(T,\hat{\mu}_B)} = r_{42}^{B,0} + \hat{\mu}_B^2 r_{42}^{B,2} + \dots \tag{11}$$

The μ_B dependence of the $\chi_i^B(T,\hat{\mu}_B)$ can be again written in terms of the Taylor expansion:

$$\chi_{i,j,k}^{BQS}(\hat{\mu}_B) = \chi_{i,j,k}^{BQS}(0) + \hat{\mu}_B \left[\chi_{i+1,j,k}^{BQS}(0) + q_1 \chi_{i,j+1,k}^{BQS}(0) + s_1 \chi_{i,j,k+1}^{BQS}(0)\right] \tag{12}$$

$$+ \frac{1}{2}\hat{\mu}_B^2 \left[\chi_{i+2,j,k}^{BQS}(0) + s_1^2 \chi_{i,j+2,k}^{BQS}(0) + q_1^2 \chi_{i,j,k+2}^{BQS}(0)\right. \tag{13}$$

$$\left. + 2q_1 s_1 \chi_{i,j+1,k+1}^{BQS}(0) + 2s_1 \chi_{i+1,j+1,k}^{BQS}(0) + 2q_1 \chi_{i+1,j,k+1}^{BQS}(0)\right] + \dots \tag{14}$$

$$\tag{15}$$

with

$$q_j = \frac{1}{j!}\frac{d^j \hat{\mu}_Q}{(d\hat{\mu}_B)^j}(0) \tag{16}$$

$$s_j = \frac{1}{j!}\frac{d^j \hat{\mu}_S}{(d\hat{\mu}_B)^j}(0) \tag{17}$$

We can now use the constrains $\langle n_S \rangle = 0$ and $\langle n_Q \rangle = 0.4\langle n_B \rangle$ which can be rewritten as

$$\chi_1^Q = 0.4\chi_1^B\,, \qquad \chi_1^S = 0 \tag{18}$$

to determine $r_{ij}^{B,k}$ coefficients form the equations 9, 10 and 11. However we now need to know not only the behaviour of the χ_i^B but also of derivatives with respect to μ_S and μ_Q. For now our

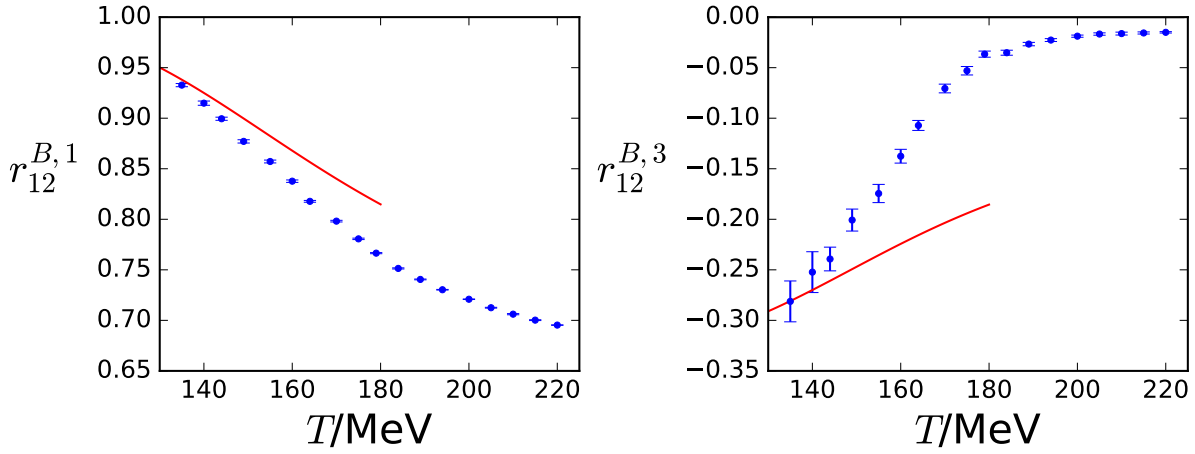

Figure 2. Taylor expansion coefficients for $\frac{M_B}{\sigma_B^2} = \frac{\chi_1^B(T,\hat{\mu}_B)}{\chi_2^B(T,\hat{\mu}_B)}$ as functions of the temperature: $r_{12}^{B,1}$ (left panel) and $r_{12}^{B,3}$ (right panel).

simulations are restricted to ensembles with finite μ_B. Therefore the μ_S and μ_Q derivatives have to be calculated directly and without the support from the fit that we used in the μ_B direction. We calculate various $\chi_{i,j,k}^{B,Q,S}$ with the appropriate values of j and k and all possible values for i so that

$$i + j + k \leq 4. \tag{19}$$

For each group of fluctuations with the same j and k we perform a fit analogous to the procedure described in section 3. This is sufficient to determine the first to $r_{ij}^{B,k}$ coefficients for all three observables. The results are shown in figure 2, 3 and 4. For higher order coefficients, higher order derivatives in μ_S and μ_Q are needed. The direct measurements have a rapidly increasing error with each derivative and very large statistics would be needed to improve our calculations in that manner. Another possibility would be add ensembles with finite μ_S and μ_Q and do a similar fit as for the μ_B direction. This approach has been used in [19].

5. Error Analysis

For a reliable comparison between experimental measurements and theoretical calculations, the error estimate is an important ingredient. Our statistical error is estimated through the jackknife method. For our systematic error there are several sources. We determine our systematic error by the histogram method described in [26], where each analysis is weighted with the Akaike information criteria. We include the influence of the number of points in the μ_B direction, by either including or ignoring the data from our highest value of μ_B. A very important source for our systematic error is the influence of the higher order contributions in μ_B. This effect was estimated by adding the higher order terms with pre-factors ϵ_1 and ϵ_2 as described in Section 3. We consider 1000 different ϵ pairs and add the different analyses to our histogram. The width of the histogram using Akaike weights corresponding to the fit quality gives the systematic errors for the fit coefficients, and from the same histogram we obtain the posterior distributions for ϵ_1. The physical quantities that are constrained only by the posterior distribution are plotted with green symbols.

These histograms are built independently for each number (j and k) of μ_S and μ_Q derivatives. When calculating the systematic for the cumulants (see section 4) we need to calculate different combinations from the available analyses. We will always take the fluctuations from the same

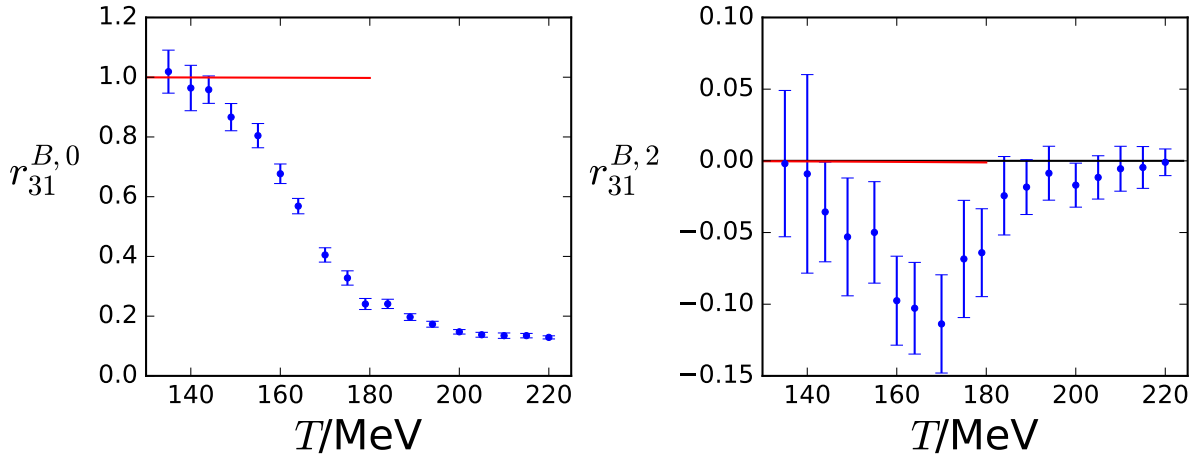

Figure 3. Taylor expansion coefficients for $\frac{S_B\sigma_B^3}{M_B} = \frac{\chi_3^B(T,\hat{\mu}_B)}{\chi_1^B(T,\hat{\mu}_B)}$ as functions of the temperature: $r_{31}^{B,0}$ (left panel) and $r_{31}^{B,2}$ (right panel).

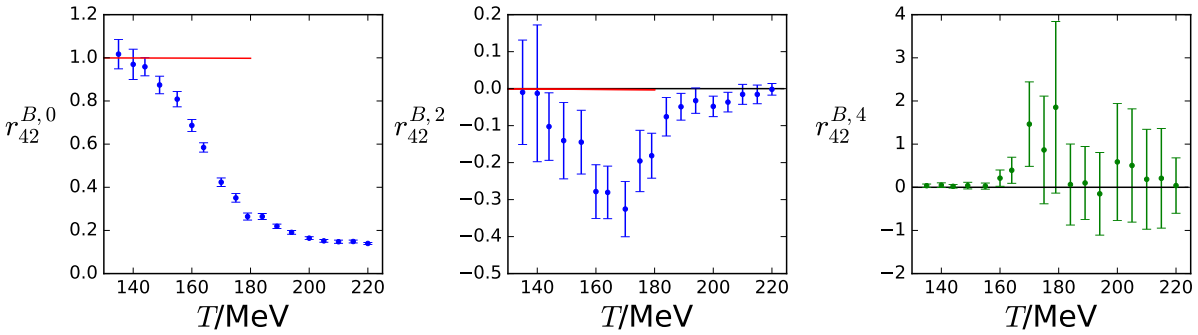

Figure 4. Taylor expansion coefficients for $\kappa_B\sigma_B^2 = \frac{\chi_4^B(T,\hat{\mu}_B)}{\chi_2^B(T,\hat{\mu}_B)}$ as functions of the temperature: $r_{42}^{B,0}$ (left panel) $r_{42}^{B,2}$ (middle panel), $r_{42}^{B,4}$ (right panel). The latter is not obtained independently, but by means of the prior ansatz (see text): for this reason, we plot it in green.

channel from the same analysis. However we have 15 channels and 2000 analyses in each resulting in 2000^{15} combinations, which would be a very large computational effort. Instead we determine 1000 different combinations via important sampling:

(i) For each channel we draw a random number r from a uniform distribution between zero and one

(ii) We add the normalized weights from our 2000 different analyses to the sum $s \geq r$ with the nth analysis

(iii) We take for this combination the nth analysis and proceed to the next channel

In this way, $\mathcal{O}(100)$ random combinations of χ_{ijk}^{BSQ} results already give convergence for each discussed quantity and its error bar. For the results in this paper we used 1000 such random combinations. This procedure assumes that between different j, k pairs the prior distribution is uncorrelated.

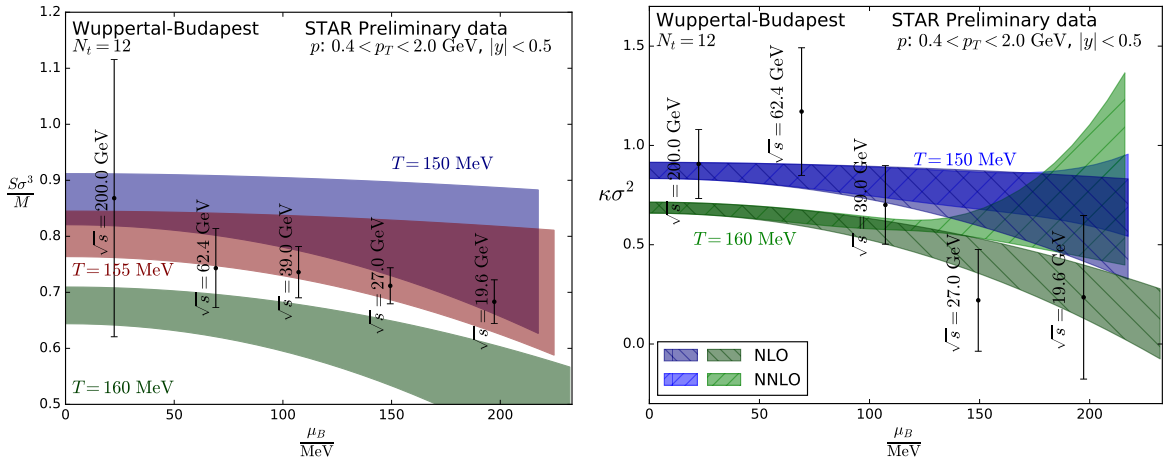

Figure 5. $S_B\sigma_B^3/M_B$ (left panel) and $\kappa_B\sigma_B^2$ (right panel) extrapolated to finite chemical potential. The left panel is extrapolated up to $\mathcal{O}(\hat{\mu}_B^2)$. In the right panel, the darker bands correspond to the extrapolation up to $\mathcal{O}(\hat{\mu}_B^2)$, whereas the lighter bands also include the $\mathcal{O}(\hat{\mu}_B^4)$ term.

6. Conclusion

We have calculated the baryon number fluctuation as well as several diagonal and non-diagonal fluctuations of electric charge, baryon number and strangeness up to sixth-order on a $48^3 \times 12$ lattice. The analysis has been performed simulating the lower order fluctuations at eight different values of zero and imaginary chemical potential μ_B, and extracting the higher order fluctuations as derivatives of the lower order ones at $\mu_B = 0$. The chemical potentials for electric charge and strangeness have both been set to zero in the simulations. From these fluctuations, we have constructed ratios of baryon number cumulants as a functions of T and μ_B, by means of a Taylor series which takes into account the experimental constraints $\langle n_S \rangle = 0$ and $\langle n_Q \rangle = 0.4\langle n_B \rangle$. These ratios qualitatively explain the behavior observed in the experimental measurements by the STAR collaboration as functions of the collision energy.

Acknowledgments

This project was funded by the DFG grant SFB/TR55. This work was supported by the Hungarian National Research, Development and Innovation Office, NKFIH grants KKP126769 and K113034. An award of computer time was provided by the INCITE program. This research used resources of the Argonne Leadership Computing Facility, which is a DOE Office of Science User Facility supported under Contract DE-AC02-06CH11357. The authors gratefully acknowledge the Gauss Centre for Supercomputing e.V. (www.gauss-centre.eu) for funding this project by providing computing time on the GCS Supercomputer JUQUEEN[27] at Jülich Supercomputing Centre (JSC) as well as on HAZELHEN at HLRS Stuttgart, Germany. This material is based upon work supported by the National Science Foundation under grants no. PHY-1654219 and OAC-1531814 and by the U.S. Department of Energy, Office of Science, Office of Nuclear Physics, within the framework of the Beam Energy Scan Theory (BEST) Topical Collaboration. C.R. also acknowledges the support from the Center of Advanced Computing and Data Systems at the University of Houston.

References

[1] Aoki Y, Endrodi G, Fodor Z, Katz S D and Szabo K K 2006 *Nature* **443** 675–678 (*Preprint* hep-lat/0611014)
[2] Aoki Y, Borsanyi S, Durr S, Fodor Z, Katz S D, Krieg S and Szabo K K 2009 *JHEP* **06** 088 (*Preprint* 0903.4155)
[3] Borsanyi S, Fodor Z, Hoelbling C, Katz S D, Krieg S, Ratti C and Szabo K K (Wuppertal-Budapest) 2010 *JHEP* **09** 073 (*Preprint* 1005.3508)
[4] Bhattacharya T *et al.* 2014 *Phys. Rev. Lett.* **113** 082001 (*Preprint* 1402.5175)
[5] Bazavov A *et al.* 2012 *Phys. Rev.* **D85** 054503 (*Preprint* 1111.1710)
[6] Allton C R, Ejiri S, Hands S J, Kaczmarek O, Karsch F, Laermann E, Schmidt C and Scorzato L 2002 *Phys. Rev.* **D66** 074507 (*Preprint* hep-lat/0204010)
[7] Allton C R, Doring M, Ejiri S, Hands S J, Kaczmarek O, Karsch F, Laermann E and Redlich K 2005 *Phys. Rev.* **D71** 054508 (*Preprint* hep-lat/0501030)
[8] Gavai R V and Gupta S 2008 *Phys. Rev.* **D78** 114503 (*Preprint* 0806.2233)
[9] Basak S *et al.* (MILC) 2008 *PoS* **LATTICE2008** 171 (*Preprint* 0910.0276)
[10] Kaczmarek O, Karsch F, Laermann E, Miao C, Mukherjee S, Petreczky P, Schmidt C, Soeldner W and Unger W 2011 *Phys. Rev.* **D83** 014504 (*Preprint* 1011.3130)
[11] Karsch F 2012 *Central Eur. J. Phys.* **10** 1234–1237 (*Preprint* 1202.4173)
[12] Bazavov A *et al.* 2012 *Phys. Rev. Lett.* **109** 192302 (*Preprint* 1208.1220)
[13] Borsanyi S, Fodor Z, Katz S D, Krieg S, Ratti C and Szabo K K 2013 *Phys. Rev. Lett.* **111** 062005 (*Preprint* 1305.5161)
[14] Borsanyi S, Fodor Z, Katz S D, Krieg S, Ratti C and Szabo K K 2014 *Phys. Rev. Lett.* **113** 052301 (*Preprint* 1403.4576)
[15] Stephanov M A, Rajagopal K and Shuryak E V 1999 *Phys. Rev.* **D60** 114028 (*Preprint* hep-ph/9903292)
[16] Cheng M *et al.* 2008 *Phys. Rev.* **D77** 014511 (*Preprint* 0710.0354)
[17] Borsanyi S, Fodor Z, Guenther J N, Katz S K, Szabo K K, Pasztor A, Portillo I and Ratti C 2018 (*Preprint* 1805.04445)
[18] Guenther J N, Bellwied R, Borsanyi S, Fodor Z, Katz S D, Pasztor A, Ratti C and Szab K K 2017 *Nucl. Phys.* **A967** 720–723 (*Preprint* 1607.02493)
[19] D'Elia M, Gagliardi G and Sanfilippo F 2017 *Phys. Rev.* **D95** 094503 (*Preprint* 1611.08285)
[20] Bonati C, D'Elia M, Negro F, Sanfilippo F and Zambello K 2018 (*Preprint* 1805.02960)
[21] McNeile C, Davies C T H, Follana E, Hornbostel K and Lepage G P 2010 *Phys. Rev.* **D82** 034512 (*Preprint* 1004.4285)
[22] Bellwied R, Borsanyi S, Fodor Z, Guenther J, Katz S D, Ratti C and Szabo K K 2015 *Phys. Lett.* **B751** 559–564 (*Preprint* 1507.07510)
[23] Roberge A and Weiss N 1986 *Nucl. Phys.* **B275** 734–745
[24] Akaike H 1992 *Information theory and an extension of the maximum likelihood principle* (Springer)
[25] Adamczyk L *et al.* (STAR) 2014 *Phys. Rev. Lett.* **112** 032302 (*Preprint* 1309.5681)
[26] Durr S *et al.* 2008 *Science* **322** 1224–1227 (*Preprint* 0906.3599)
[27] Jülich Supercomputing Centre 2015 *Journal of large-scale research facilities* **A1** 1